SIMULATION OF THE OPEN-HOLE TENSILE RESPONSE OF COMPOSITE LAMINATES USING A COMBINED DISCRETE AND CONTINUUM DAMAGE APPROACH

Mina Shahbazi[1], Reza Vaziri[1]

[1] Composites Research Network, The University of British Columbia, Vancouver, Canada
mina@composites.ubc.ca, reza.vaziri@ubc.ca

Keywords: Damage Progression, Open-Hole Tensile Test, Nonlocal Continuum Damage Model, Cohesive Zone Model, Explicit FEM

ABSTRACT

In this study, an efficient combination of continuum and discrete damage mechanics based approaches is used to model the interacting effect of delamination and intra-laminar damage modes in notched composite laminates subjected to tensile loading [1]. Delamination is the only mode of damage captured by a discrete approach while all intra-laminar forms of damage are modelled using a nonlocal continuum damage approach.

A series of open-hole specimens that have been tested under tensile loading [2] are simulated using the proposed approach. The specimens are made of quasi-isotropic IM7/8552 carbon fibre/epoxy laminates with varying hole diameter, ply and laminate thickness while keeping the ratios of the hole diameter to specimen width and length constant. The current approach is shown to capture the dominant failure mechanisms as well as the overall behaviour, including the size and layup effect on the notched strength of the laminate.

1 INTRODUCTION

Reliable prediction of the inelastic behaviour of laminated composite materials requires that the computational model be able to capture the interaction of several failure/damage mechanisms including matrix cracking, fibre breakage, splitting and delamination. The accurate prediction of the onset and propagation of certain discrete damage modes (e.g. splitting and delamination), is critical in predicting the progressive damage response of the laminate up to its ultimate failure.

In a continuum approach, damage is considered to occur as a result of multiple damage modes with no single isolated crack that dominates the zone of damage. In such cases one may consider the effect of multiple micro-cracks smeared into a locally homogeneous continuum field. An example of this approach is the sub-laminate based material model that was first developed at UBC known as CODAM [3]. More recently, the second generation of this model (CODAM2) has been introduced [4] with a nonlocal regularization scheme to address both the mesh size and orientation dependencies of the numerical solution. A built-in form of this material model is available in the commercial finite element software package, LS-DYNA, as MAT219. A practical methodology for calibrating these models has also been developed [5].

The material constants required as input for this model are the initiation and saturation values of the equivalent strains that drive each mode of damage. This material model has been originally developed to represent the effective behaviour of a sublaminate where the initiation and saturation strain values are deduced from the experimentally characterized strain-softening curves and the fracture energy of the sublaminate rather than those of the individual plies [6]. This approach is applicable when the extent of delamination is relatively minor and the material building block can be considered to be a

sublaminate with an effective stress-strain behaviour representing the smeared effect of intra-laminar damage modes.

For cases where failure is dominated by formation of discrete macro-cracks that lead to a relatively large damage zone, continuum damage models fail to correctly describe the propagation of damage through the structure. For instance delamination, which may be accompanied by intra-laminar splitting (longitudinal matrix cracks) in the proximity of notches or discontinuities, plays an important role in blunting the stress concentration at the notch tip and thus altering the load path within the laminate.

When there is a need to model delamination that stems from transverse matrix cracks in the neighbouring plies of the delaminated interface [7], accurate estimation of the onset of matrix cracking becomes important. It is generally acknowledged that formation of transverse matrix cracks in a ply is dependent on the constraining effects of its neighbouring plies in the laminate and that thicker transverse plies are more prone to matrix cracking and delamination [8,9]. Based on these observations, some researchers differentiate between the behaviour of a unidirectional lamina and that of a lamina embedded within a laminate [10-12].

In this work, the original CODAM2 material model, which was previously used to describe the macroscopic (smeared) damage behaviour of a laminate, is enhanced and used in a mesoscopic form to capture the progressive intra-laminar damage behaviour in individual plies of the laminate interspersed with cohesive elements. In the mesoscopic version of CODAM2, Hashin's failure criteria [13-15] are used to identify the onset of intra-laminar matrix and fibre damage modes. The constraining effect of the immediate neighbouring plies as well as the ply thickness effect on matrix cracking is also considered through an approximate analytical model based on combination of fracture mechanics and shear lag theories introduced by Zhang et al. [16,17]. The enhanced CODAM2 material model formulation is implemented as a user-defined material model (UMAT) in the commercial finite element software package, LS-DYNA [18].

From the numerical point of view, the explicit modelling of delamination as a macro-crack that separates the plies allows for accurate redistribution of stresses. Moreover, it enables the transverse matrix cracks and splits in the separated plies to grow independently of the remainder of the laminate. Therefore, in combination with the continuum approach to capture the intra-laminar damage, a mixed-mode cohesive-based contact formulation available in LS-DYNA [18] is used to model the delamination between all dissimilar plies. Through a 3D stress analysis and synchronization of the onsets of delamination and matrix damage, we are able to obtain a reasonably detailed response of the material in terms of intra-laminar and inter-laminar damage modes in a computationally efficient way.

In a previous study [1], this methodology was used for predicting the progressive damage in over-height compact tension (OCT) test geometries involving quasi-isotropic laminates of IM7/8552 carbon fibre/epoxy (CFRP) with two different stacking sequences: (i) a dispersed layup of thin layers ($[90/45/0/-45]_{4S}$) [6], and (ii) a lumped (ply-scaled) layup of thick layers ($[454/904/-454/04]_{S}$) [19]. The predictions showed that the current methodology can correctly capture the distinct nature of damage modes in the above mentioned laminate layups. While the damaged zone in dispersed laminate includes minor delamination and is dominated by fibre breakage, the blocked-ply laminate shows individual isolated macro-cracks and splits with large delamination zones. The global response of the laminates in terms of force vs pin-opening displacement (POD) was also found to be in agreement with the experiments.

In this paper a series of open-hole specimens that have been tested under tensile loading at the University of Bristol [2] will be modeled using the proposed approach. The specimens are made of IM7/8552 CFRP laminates with a quasi-isotropic lay-up and various hole diameters, ply and laminate thicknesses while keeping the hole diameter to specimen width and length ratios constant.

2 METHODOLOGY

In layups and loading geometries that are marked by formation of large splits followed by discrete macro-delamination between the plies, fibre breakage will be delayed and the laminate stiffness reduction is mostly governed by the initiation of splits and delamination. Given the sensitivity of these types of response to initiation of damage (mainly matrix cracking and the ensuing delamination), it is important to have damage criteria that consider the effect of ply thickness and constraining effect of the neighbouring plies on the initiation of matrix cracking. The interactive effect of transverse normal and shear stress components on matrix cracking combined with the inherent non-linear shear stress-strain response of unidirectional composites necessitates the use of stress-based criteria to signal matrix damage. To this end, the CODAM2 material model formulation was enhanced and applied at the mesoscopic level of individual plies [1]. In what follows some of the key features of the model will be reviewed.

Hashin's failure criteria [13,14] in which the failure surface is expressed in terms of an effective stress reaching a critical state is used for initiation of intra-laminar matrix and fibre damage modes. Moreover, the effect of ply thickness and constraint from the stiffness of neighbouring plies on transverse matrix cracking are taken into account using the analytical expressions obtained from the shear-lag theory [16,17].

Damage parameters in the current material model, written in terms of the fibre and matrix equivalent strain components, ε_1^{eq} and ε_2^{eq} are summarized in Table 1. Note that in the equivalent strain equation for matrix damage, γ_{12}^e is the elastic part of the in-plane shear strain in cases where the in-plane shear behaviour is non-linear. It is well-known that the in-plane shear response in most unidirectional laminates is nonlinear and inelastic. Therefore, a nonlinear in-plane shear stress vs strain constitutive behaviour has been implemented in the enhanced formulation of CODAM2 material model. Since progression of damage is driven by the reduction in elastic stiffness of the material, only the elastic component of the total shear strain (γ_{12}^e) is taken into account in the equivalent strain formulation used for tracking matrix crack propagation.

Using the nonlocal averaging feature available in LS-DYNA, the averaged equivalent strains, $\overline{\varepsilon}_\alpha^{eq}$ $(\alpha = 1,2)$, at each point are obtained by a weighted average of the local equivalent strains, ε_α^{eq}, of the neighbour points that are located within a circular region of radius, *r*, centered at that point. The nonlocal equivalent strains are then used to calculate the damage parameters from the onset of damage (initiation strain), when the damage parameter is zero, all the way to saturation of damage when the damage parameter reaches unity.

The initiation values of the equivalent strain components are determined at the instant when the failure criterion for each damage mode is satisfied. In other words, when the Hashin's criterion for fibre damage and matrix damage are satisfied (i.e. $F_1 = 1$ and $F_2 = 1$, respectively, where F_1 and F_2 are non-dimensional functions of appropriate stresses), the initiation of damage in the strain space will be set accordingly (see Table 1).

Damage mode	Equivalent strains	Equivalent strains at initiation of damage
Fibre damage	$\varepsilon_1^{eq} = \lvert\varepsilon_{11}\rvert$	$\varepsilon_1^{i} = \overline{\varepsilon}_1^{eq}\big\rvert_{@F_1=1}$
Matrix damage	$\varepsilon_2^{eq} = \sqrt{(\varepsilon_{22})^2 + (\gamma_{12}^e)^2}$	$\varepsilon_2^{i} = \overline{\varepsilon}_2^{eq}\big\rvert_{@F_2=1}$

Table 1. The equivalent strains that drive the intra-laminar damage modes and their initiation values

The saturation values for the equivalent strain corresponding to the matrix damage mode are calculated based on the corresponding intra-laminar matrix fracture energy and the transverse and shear stress components at the onset of damage. For this purpose, an equivalent stress corresponding to the equivalent matrix strain is defined as follows:

$$\sigma_2^{eq} = \frac{(\sigma_{22}\varepsilon_{22} + \tau_{12}\gamma_{12}^e)}{\sqrt{(\varepsilon_{22})^2 + (\gamma_{12}^e)^2}} \tag{1}$$

The value of this equivalent stress at the initiation of matrix damage mode, $T = \sigma_2^{eq}\big|_{@F_2=1}$, is used to estimate the saturation strain for matrix damage such that for a bilinear strain-softening curve:

$$\varepsilon_2^s = \frac{2g_2^f}{T} \tag{2}$$

where g_2^f is the intra-laminar matrix fracture energy density (i.e. area under the stress-strain curve). The value of g_2^f is related to the intra-laminar matrix fracture energy, G_2^f, through a characteristic length, h_c, such that $g_2^f = G_2^f / h_c$. In this nonlocal continuum damage model, the characteristic length h_c is proportional to the radius, *r*, used for nonlocal averaging. Based on numerical case studies the relationship between *r* and h_c is found to satisfy the following inequality: $0.65r < h_c < 1.3r$. The value of *r* is chosen to be large enough to account for all the elements within the experimentally measured height of the damaged-zone. The saturation value for the fibre equivalent strain is also calculated as follows:

$$\varepsilon_1^s = \frac{2g_1^f}{X} \tag{3}$$

where X is the ply longitudinal (fibre direction) strength and g_1^f is the intra-laminar fibre fracture energy density. The estimation of g_1^f in nonlocal-averaging approach follows a similar approach to that used for the matrix damage mode.

2.1 Effect of ply thickness and confinement on matrix damage initiation

It is well known that the transverse matrix crack density and the corresponding stiffness reduction of a cracked ply can be influenced by the thickness of that ply and the stiffness of the adjacent constraining plies. Experimental studies show higher transverse tensile and shear strengths for a 90° ply that is constrained by plies with different fibre orientations in a laminate, when compared to the strength of an unconfined unidirectional 90° laminate (see for example [8,9]). There have been many studies to determine the in-plane stiffness reduction and the in-situ strengths of cracked plies using experimental and analytical methods. Among these methods, a simple method that has been applied is based on the shear lag theory [16,17].

The total strain energy associated with matrix cracking in the cracked, constrained layer can be related to the rate of stiffness loss under the in-situ constraint condition. From the knowledge of the in-plane stiffness of the cracked lamina for a given crack density, the energy release rate can then be derived as a function of the applied stresses and the rate of stiffness reduction.

Therefore, the in-situ tensile strength (Y_T^{is}) and shear strength (S_L^{is}) of the layer are determined as a limit of the energy release rate approaching the critical fracture energy at the instant when the crack density is zero. The criterion for failure of the matrix in tension can then be expressed in terms of the ply stresses and in-situ strengths by replacing the strength properties in Hashin's failure criterion (for

tensile matrix cracking) with the in-situ strength properties, Y_T^{is} and S_L^{is}, obtained from the shear lag theory [1].

2.2 Inter-laminar damage

As mentioned before in our combined continuum and discrete damage modeling approach, the inter-laminar damage mode (i.e. delamination) is modelled using a discrete approach. The potential delamination interfaces between the plies can be modelled using a cohesive-based tie-break contact known as *CONTACT_AUTOMATIC_ONE_WAY_SURFACE_TO_SURFACE_TIEBREAK in LS-DYNA, which follows a bilinear traction-separation law with quadratic mixed-mode delamination criterion. The separation between nodal points of the elements from two neighbouring plies is triggered by a damage parameter when it reaches a value of one. The damage starts when the total relative mixed mode displacement δ_m between the nodes of elements from two neighbouring plies exceeds the mixed-mode damage initiation displacement, δ_m^0. This critical displacement is a function of the maximum inter-laminar normal and shear tractions,, $t_{\max}^N$ and $t_{\max}^S$, respectively. The mixed-mode traction-separation law is controlled by a damage parameter defined in terms of the mixed-mode displacement, δ_m, written as a function of separations in the normal and tangential directions (modes I and II). The saturation of this damage parameter is defined based on a mixed-mode power law used as a damage growth criterion. The details of this formulation are provided in the user manual of LS-DYNA [18].

The accurate prediction of the singular state of inter-laminar stresses in finite element methods requires an extremely fine mesh which is quite often impractical. In order to capture the onset of delamination using a coarse finite element mesh, the inter-ply strength values are scaled down based on the value of the operative inter-laminar stresses at the instant when matrix damage in the neighbouring ply (plies) is deemed to have occurred. The inter-laminar fracture energy values in mode I and mode II are maintained constant. The details of this process are presented in [1].

3 MATERIALS AND EXPERIMENTS

The experimental setup and results are presented in detail by Green et al. [2]. Key features and findings are recounted here to facilitate comparison with the current numerical results. The material used was based on unidirectional IM7/8552 CFRP prepreg system supplied by Hexcel. The nominal ply thickness is 0.125mm. This is the same material considered in the World Wide Failure Exercise and for which the standard material properties can be found in Kaddour et al. [20].

The specimen design consists of a gauge section of constant cross-sectional area, with width *W*, thickness *t* and length *L*, and a centrally located hole of diameter *D*. At either end of the gauge section is a gripping region. The specimen gauge length has constant ratios of *W/D*=5 and *L/D*=20 for all specimen sizes. A quasi-isotropic laminate with stacking sequence $[45_m/90_m/45_m/0_m]_{ns}$ was used, with 0^O being in the direction of the applied loading. The product of m and n is equal to the laminate thickness (i.e. *m, n* = 1 for a 1 mm thick laminate; *m* = 2, *n* = 1 or m = 1, *n* = 2 for a 2 mm thick laminate; etc.). Increasing *m* increases the number of plies of the same orientation blocked together, i.e. it increases the effective ply thickness which is referred to as ply-level scaling. Increasing *n* keeps a constant ply thickness, but increases the laminate thickness by increasing the number of sublaminates that are present. This is referred to as sublaminate-level scaling.

The in-plane dimensions of the baseline specimen are scaled by a factor of 2 each time up to a maximum of 4. The minimum hole diameter used is 3.175mm. The failure load was taken as being the first significant (greater than 5%) load drop on the load-displacement curve, which corresponded to either fibre failure or extensive delamination throughout the gauge section. The failure strength was obtained by dividing the failure load by the un-notched cross-sectional area of the specimen.

4 NUMERICAL SIMULATIONS

To reduce the model size, only the gauge length was modelled. Also, due to symmetry of the lay-ups, only half of the thickness of the laminates was modelled with plane symmetric boundary conditions applied at the mid-plane of the laminates. Based on the proposed method, each individual ply is modelled with one under-integrated thick-shell element (ELFORM = 5 in LS-DYNA) in the thickness direction. For each layer of elements, 2 integration points through the thickness are considered. Moreover, the CODAM2 material model was assigned to each layer of elements with its specific ply orientation. Both blocked-ply (n = 1 and $m \geq 1$) and dispersed-ply (m = 1, $n \geq 1$) layups were modelled using this approach. A tiebreak contact with cohesive-based damage formulation (Option 9 in LS-DYNA) was defined between the plies to simulate delamination.

The mesh size for a region close to the hole is about 0.25mm starting from the hole boundary and increasing gradually towards the free edges of the specimen. The mesh size along the length of the specimen increases to 1.5mm at the two ends of the specimen where the load is applied. A pair of prescribed displacement controlled loading with constant rates of 317.5mm/s, 635mm/s and 1270mm/s was applied on the two ends of the specimens with 3.175mm, 6.35mm and 12.7mm hole size. A stiffness based hourglass control (Type 4 in LS-DYNA) was used with stiffness coefficient of 0.6 to prevent zero energy mode shapes.

The predicted and experimental results for the strength of the ply-scaled specimens with D=3.175mm and D=6.35mm are shown in Figure 1a overlaid with the average experimental values for the two hole sizes. The load values are divided by the un-notched cross-sectional area of the specimen to visualize the size effect. It can be seen that the size effect with respect to the ply thickness is captured well with the proposed numerical model. Without the size effect the maximum load would have scaled linearly with the thickness resulting in a constant maximum far-field stress.

The predicted stress values and the corresponding experimental values for thin-ply (0.125mm) and thick-ply (0.5mm) laminates with total thickness of 4mm are plotted in Figure 1b as a function of the hole diameter. For thin-ply laminates, the fibre breakage is the dominant damage mechanism for all specimen scales. The increase in hole size leads to a decrease in strength due to an increase in the in-plane dimensions. This is consistent with the classical hole size effect as expected based on fracture mechanics. Among these models, one can mention the Whitney-Nuismer hole size model [21]. For thick plies, however, the failure is dominated by delamination in all the specimen scales. The hole-size effect in thick-ply specimens shows the opposite trend to what is observed in thin plies. An increase in the in-plane dimensions leads to an increase in the strength. In [22], this behaviour is attributed to the fact that in larger coupons the ligament (i.e. the space between the hole edge and the specimen's free edge along the specimen width) is larger and the propagation of delamination across the whole width of the specimen requires more energy.

As an example, the predicted load-displacement curves for 4mm thick specimens with D=6.35mm made of single and quadruple ply thickness are shown in Figure 2a. It is seen that for single ply laminates (t_p=0.125mm) the behaviour is almost linear until an abrupt failure occurs. The failure corresponds to fibre breakage in the 0^o plies as shown in Figure 2c for a post-peak time step as indicated by red square marker in Figure 2b. Similar damage patterns are also predicted for D=3.175mm and D=12.7mm hole size specimens with 0.125mm thick plies which are not shown here.

For thick-ply laminates (t_p = 0.5mm), however, the stiffness of the laminate gradually decreases before the load drop which corresponds to the failure point (see Figure 2a). The failure is the result of the propagation of delamination and its migration from one interface to the other. In thick-ply laminates, the failure is dominated by delamination. Based on experimental observations [2], the stiffness degradation begins with matrix cracking in the outer 45^o layer along the edges of the hole and then propagates across the plies and interfaces until the delamination at the -45/0 interface crosses the whole width of the specimen which corresponds to the first load drop. The simulation results of thick-

ply specimens, shown in Figure 2b, and 2c are in good qualitative agreement with the experimental observations and the predicted evolution of internal ply cracking and associated interface delamination. On the global stress-displacement curve, there is a gradual decrease in the slope which is related to the progression of transverse matrix cracks and delamination. Figure 3 also shows the damage pattern in all the plies of the thick-ply laminate (t_p = 0.5mm) with D=6.35mm including the matrix damage and delamination which are qualitatively in agreement with the experimental results.

The proposed modelling approach has been able to capture the dominant failure mechanisms as well as the overall behaviour of the laminate in a computationally efficient manner. As shown in Figure 1, the predicted size effects associated with varying ply thickness (represented by the ply-scale parameter m) and in-plane size of the specimen (represented by the hole diameter, D) are found to be in general agreement with the experimentally-obtained results.

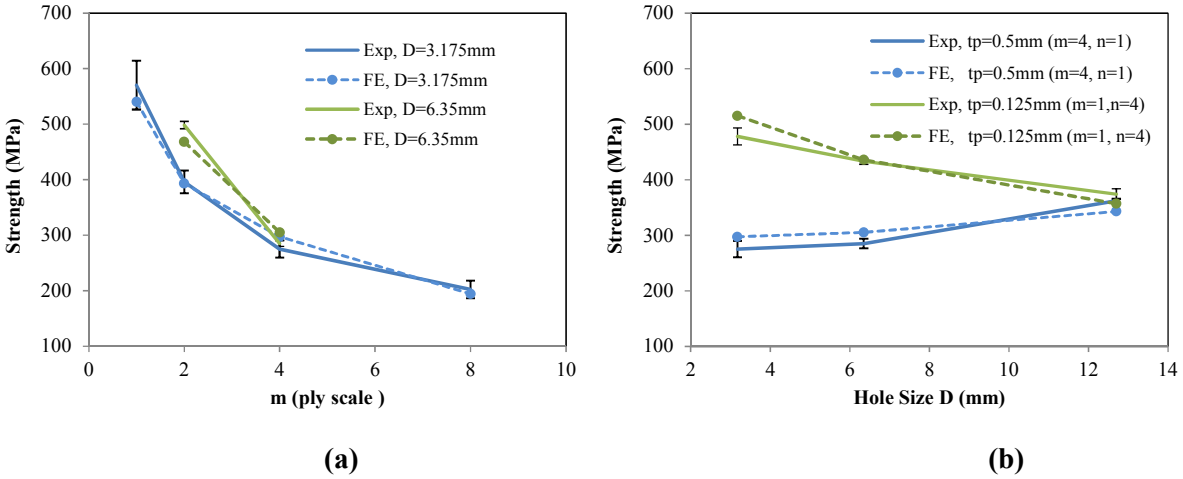

Figure 1. Comparison of the predicted and measured strengths of scaled quasi-isotropic, open-hole tensile specimens with $[45_m/90_m/-45_m/0_m]_{ns}$ layups showing: (a) the effect of ply thickness (varying m with n=1) for two hole diameters of D=3.175mm and 6.35mm; and (b) the effect of specimen size for a 4-mm thick laminate with ply-scaled (m=4, n=1) and sub-laminate scaled (m=1, n=4) layups

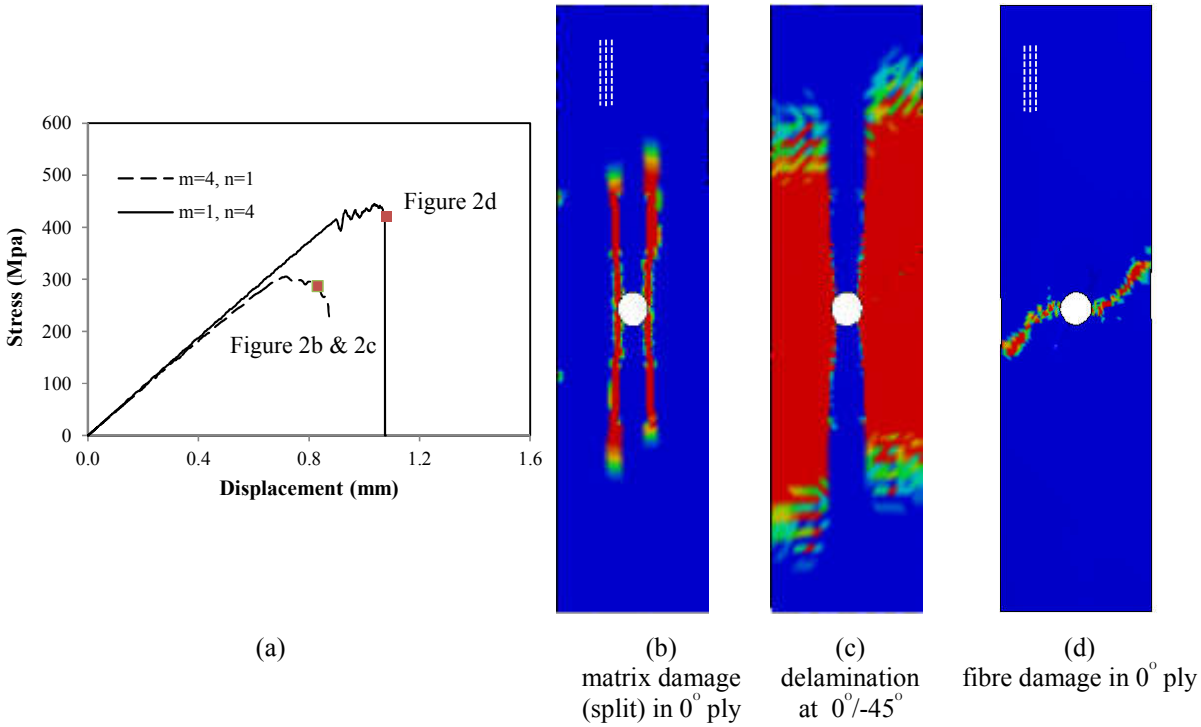

Figure 2. (a) Predicted global stress-displacement curves for 4mm thick specimens with D=6.35mm hole size made of single and quadruple ply thickness, (b) split patterns in the 0^0 ply, (c) delamination at 0^0/-45 interface as the dominant failure mechanisms of thick-ply laminate shown for a post-peak time step, and (d) fibre damage in the 0^0 ply as the dominant failure mechanism of thin-ply laminate shown for a representative post-peak time step

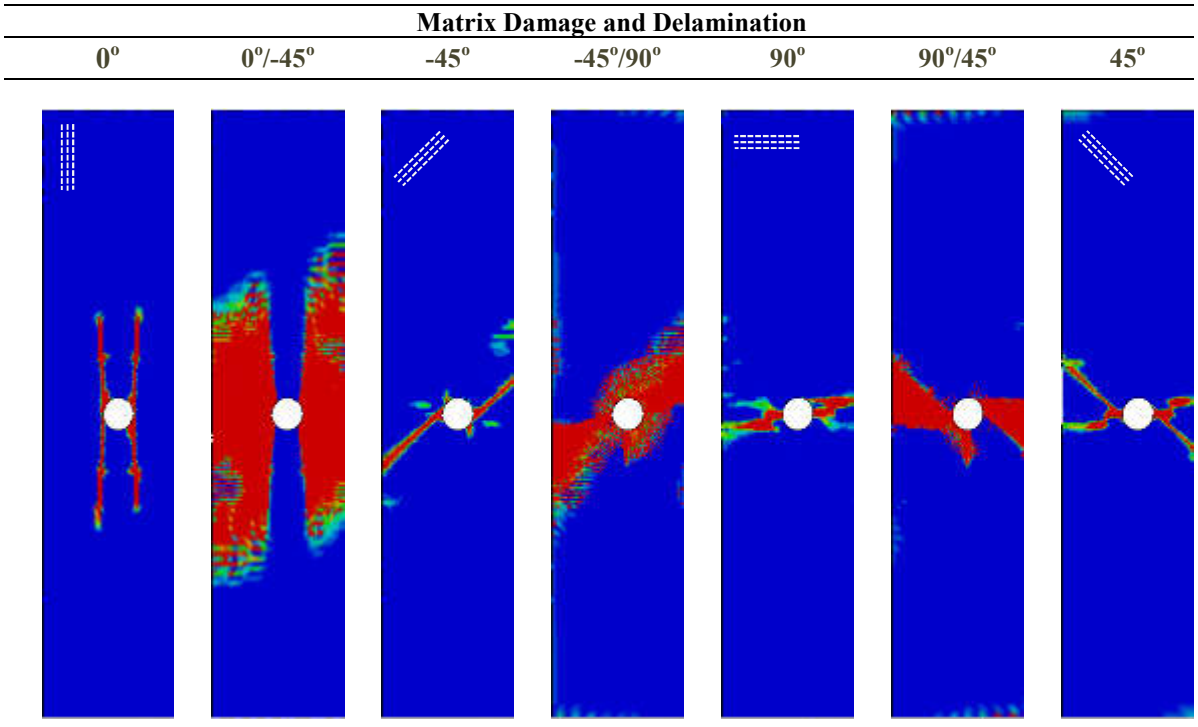

Figure 3. State of matrix damage for all plies and delamination at each interface for $[45_4/90_4/-45_4/0_4]_s$ specimen with D=6.35mm at a time step after the first load drop as shown in Figure 2(a) by red square mark.

5 SUMMARY AND CONCLUSIONS

An effective combination of continuum damage and discrete damage modelling approach is used to predict the interacting effect of the intra-laminar and inter-laminar damage modes on the behaviour of laminate layups or geometries where delamination is a dominant damage mechanism. Use of mesoscopic CODAM2 material model in conjunction with the nonlocal averaging technique enables the prediction of major splits within the plies without the need to pre-insert discrete elements thus reducing the computational effort considerably. This methodology is promising as a virtual testing tool to capture the behaviour of different laminate layups and the sensitivity of their behaviour to the damage related parameters including the initiation and saturation of intra-laminar damage modes and their interaction with delamination.

In this study, the calibrated enhanced CODAM2 material model for IM7/8552 CFRP material system [1] is combined with cohesive type interfaces between the plies to predict damage progression in an open hole tensile test geometry. The corresponding experiments were conducted by Green et al. [2] on quasi-isotropic laminates with various ply-level and sublaminate-level scaled geometric sizes.

The predictions have been shown to capture the transition from the fibre-dominated failure mode to the matrix (delamination)-dominated mode as the thickness of plies increases. The introduction of the ply thickness effect for predicting the onset of transverse matrix cracking and the coupling between intra-laminar and inter-laminar damage are essential requirements for capturing such transition.

The model has also correctly captured the in-plane size effect for both thin- and thick-ply laminates. The in-plane size effect for the thin-ply laminates is consistent with the classical hole size effect based on classical fracture mechanics. However, for the thick-ply laminates failure is mostly dominated by matrix cracking and delamination. Therefore, the size of the ligament plays an important role in the strength of these laminates. Since the ligament size is greater in the larger coupons, the propagation of delamination across the whole width of the specimen requires more energy. Therefore, in this case, the laminate strength increases with its in-plane size.

ACKNOWLEDGEMENTS

The financial support for this work provided by the Natural Sciences and Engineering Research Council (NSERC) of Canada is gratefully acknowledged.

REFERENCES

[1] M. Shahbazi, R. Vaziri and N. Zobeiry, An Efficient Virtual Testing Framework to Simulate the Interacting Effect of Intra-laminar and Inter-laminar Damage Progression in Composite Laminates, *Proceedings of American Society for Composites 2016, Thirty-First Technical Conference, Virginia.,* 2016,.

[2] B. G. Green, M. R. Wisnom and S. R. Hallett, An experimental investigation into the tensile strength scaling of notched composites, *Composites Part A: Applied Science and Manufacturing,* **38**, 2007, pp. 867-878.

[3] K. V. Williams, R. Vaziri and A. Poursartip, A physically based continuum damage mechanics model for thin laminated composite structures, *International Journal of Solids and Structures,* **40**, 2003, pp. 2267-300.

[4] A. Forghani, N. Zobeiry, A. Poursartip and R. Vaziri, A structural modelling framework for prediction of damage development and failure of composite laminates, *Journal of Composite Materials,* **47**, 2013, pp. 2553-2573.

[5] N. Zobeiry, A. Forghani, C. McGregor, S. McClennan, R. Vaziri and A. Poursartip, Effective calibration and validation of a nonlocal continuum damage model for laminated composites, *Composite Structures*, **173**, 2017, pp. 188-195.

[6] N. Zobeiry, R. Vaziri and A. Poursartip, Characterization of strain-softening behavior and failure mechanisms of composites under tension and compression, *Composites Part A: Applied Science and Manufacturing,* **68**, 2015, pp. 29-41.

[7] WW Stinchcomb, NE Ashbaugh, Composite materials: fatigue and fracture, Astm International 1993.

[8] T. A. Sebaey, J. Costa, P. Maimí, Y. Batista, N. Blanco and J. A. Mayugo, Measurement of the in situ transverse tensile strength of composite plies by means of the real time monitoring of microcracking, *Composites Part B: Engineering,* **65**, 2014, pp. 40-46.

[9] A. Parvizi, K. W. Garrett and J. E. Bailey, Constrained cracking in glass fibre-reinforced epoxy cross-ply laminates, *Journal of Materials Science,* **13**, 1978, pp. 195-201.

[10] P. D. Soden, M. J. Hinton and A. S. Kaddour, Comparison of the predictive capabilities of current failure theories for composite laminates, *Composites Science and Technology,* **58**, 1998, pp. 1225-1254.

[11] D. L. Flaggs and M. H. Kural, Experimental Determination of the In Situ Transverse Lamina Strength in Graphite/Epoxy Laminates, *Journal of Composite Materials,* **16**, 1982, pp. 103-116.

[12] C Davila, N Jaunky, S Goswami, Failure Criteria for FRP Laminates in Plane Stress, American Institute of Aeronautics and Astronautics, 2003,.

[13] Z. Hashin, Failure Criteria for Unidirectional Fiber Composites, *Journal of Applied Mechanics,* **47**, 1980, pp. 329-334.

[14] Z. Hashin and A. Rotem, A Fatigue Failure Criterion for Fiber Reinforced Materials, *Journal of Composite Materials,* **7**, 1973, pp. 448-464.

[15] Z. Hashin, Failure Criteria for Unidirectional Fiber Composites, *Journal of Applied Mechanics,* **47**, 1980, pp. 329-334.

[16] J. Zhang, J. Fan and C. Soutis, Analysis of multiple matrix cracking in [±θm/90n]s composite laminates. Part 1: In-plane stiffness properties, *Composites,* **23**, 1992, pp. 291-298.

[17] J. Zhang, J. Fan and C. Soutis, Analysis of multiple matrix cracking in [±θm/90n]s composite laminates. Part 2: Development of transverse ply cracks, *Composites,* **23**, 1992, pp. 299-304.

[18] LS-DYNA Keyword User's Manual, (2015).

[19] X. Li, S. R. Hallett, M. R. Wisnom, N. Zobeiry, R. Vaziri and A. Poursartip, Experimental study of damage propagation in Over-height Compact Tension tests, *Composites Part A: Applied Science and Manufacturing,* **40**, 2009, pp. 1891-1899.

[20] A. S. Kaddour, M. J. Hinton, P. A. Smith and S. Li, Mechanical properties and details of composite laminates for the test cases used in the third world-wide failure exercise, *Journal of Composite Materials,* **47**, 2013, pp. 2427-2442.

[21] J. M. Whitney and R. J. Nuismer, Stress Fracture Criteria for Laminated Composites Containing Stress Concentrations, *Journal of Composite Materials,* **8**, 1974, pp. 253-265.

[22] S. R. Hallett, B. G. Green, W. G. Jiang and M. R. Wisnom, An experimental and numerical investigation into the damage mechanisms in notched composites, *Composites Part A: Applied Science and Manufacturing,* **40**, 2009, pp. 613-624.